

Reversible Loss of Bernal Stacking during the Deformation of Few-Layer Graphene in Nanocomposites

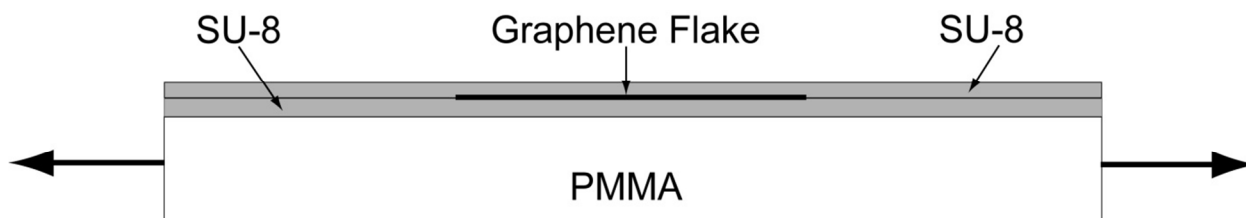
Lei Gong¹, Robert J. Young^{1*}, Ian A. Kinloch¹, Sarah J. Haigh¹, Jamie H. Warner², Jonathan A. Hinks³, Ziwei Xu⁴, Li Li⁴, Feng Ding⁴, Ibtisam Riaz⁵, Rashid Jalil⁵ and Kostya S. Novoselov⁵

¹Materials Science Centre, School of Materials and ⁵School of Physics and Astronomy, University of Manchester, Oxford Road, Manchester M13 9PL, UK, ²Department of Materials, University of Oxford, 16 Parks Road, Oxford OX1 3PH, UK, ³Department of Engineering and Technology, University of Huddersfield, Queensgate, Huddersfield, HD1 3DH, UK and ⁴Institute of Textiles and Clothing, Hong Kong Polytechnic University, Hung Hom, Hong Kong

SUPPORTING INFORMATION

S1. Deformation of Graphene Nanocomposites

In this present study we followed the effect of deformation upon the 2D band in the Raman spectra of a number of model nanocomposites consisting of exfoliated monolayer, bilayer, trilayer and few-layer graphene flakes embedded in a polymer matrix on a poly(methyl methacrylate) (PMMA) beam. The flakes were sandwiched between thin layers of cured SU-8 (spin-coated to ~300 nm thick) as shown schematically in the diagram below (not to scale).



Full details of the specimen preparation and test procedures are given elsewhere.¹⁻³ The Raman spectra were excited using a 785 nm (1.59 eV) laser with a Renishaw 2000 Raman spectrometer and obtained from the middle of a number of different flakes on the PMMA beam, with a laser power at the sample of < 1 mW. The beam was deformed in steps of ~0.05% strain to 0.4% strain (monitored using a resistance strain gauge fixed to the beam) using a four-point bending rig and then unloaded.

Two types of deformation experiments were undertaken:

- Spectra were obtained at each strain level from points on the central regions of each the flakes being monitored.
- A series of spectra were obtained at different positions along a flake of trilayer graphene to map the behaviour at different positions on the flake at different strain levels.

S1.1 Band shift in the central region of a monolayer flake

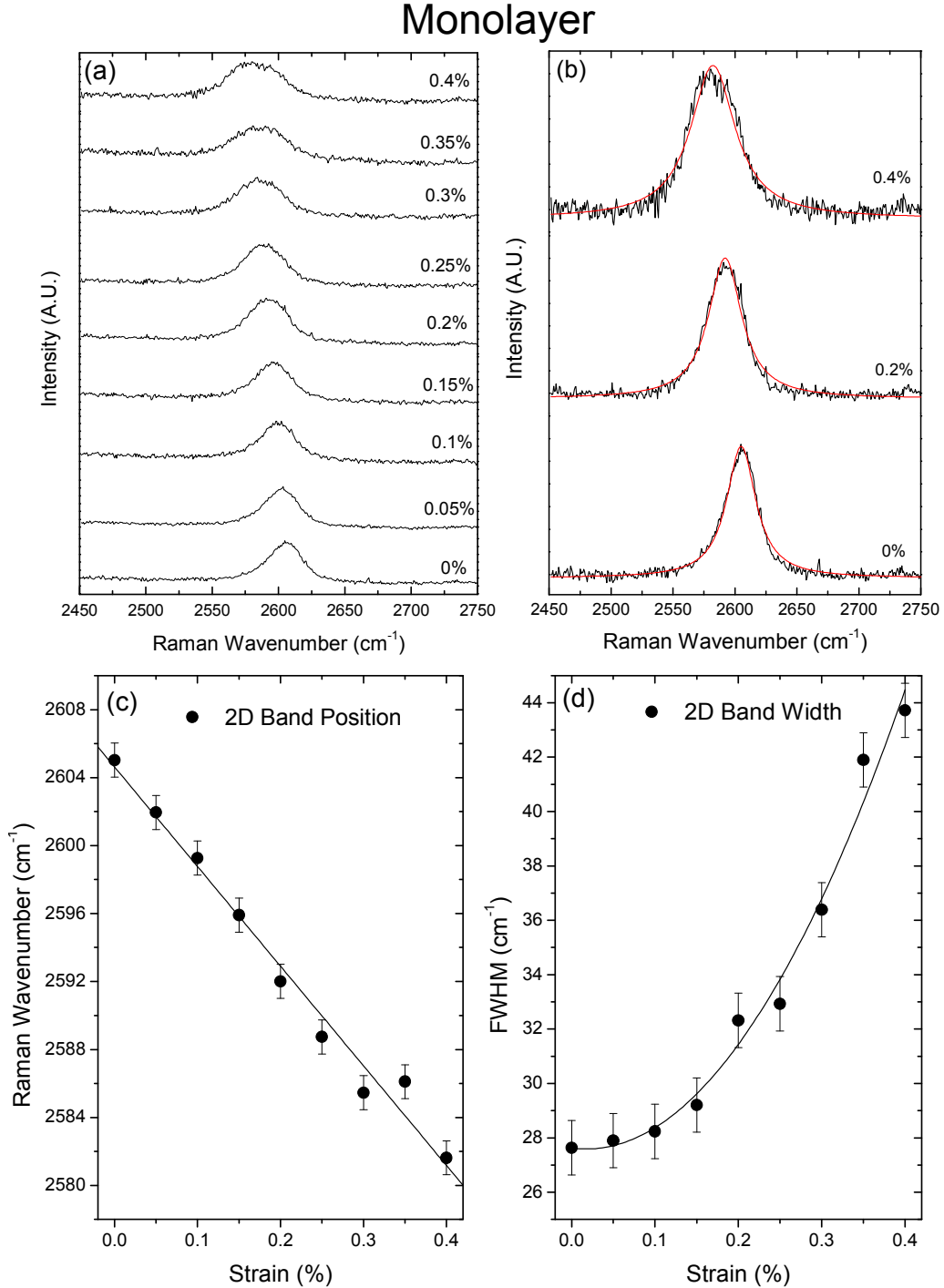


Figure S1. Shift of the 2D Raman band with strain for a graphene monolayer flake in a model nanocomposite. (a) Overall band shift for the monolayer, (b) Details of the band for the monolayer, (c) Shift with strain of the bands fitted to a single peak, (d) The variation with strain of the FWHM (full width at half maximum height) of the bands fitted to a single peak.

S1.2 Band shift in the central region of a bilayer flake

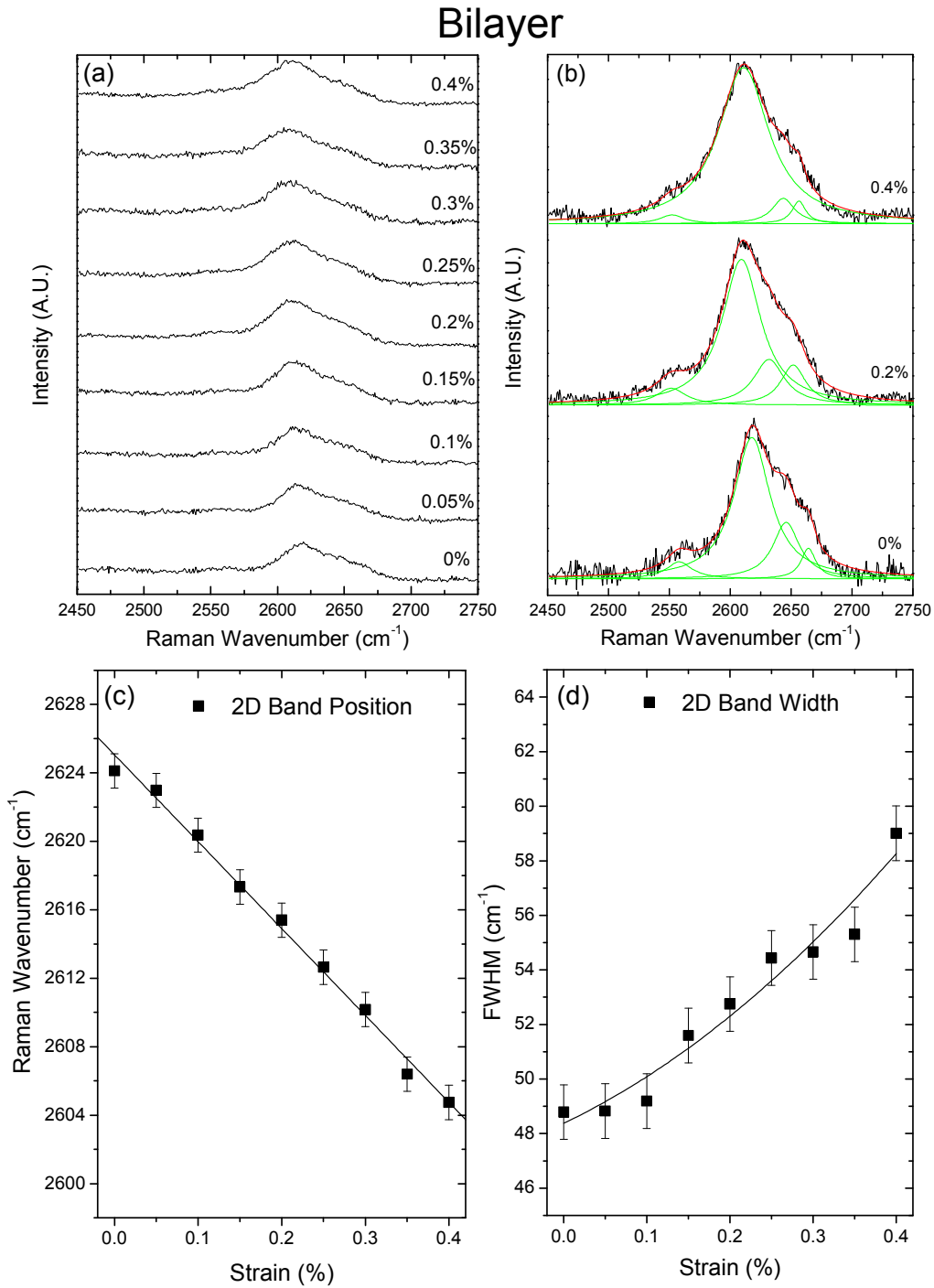


Figure S2. Shift of the 2D Raman band with strain for a graphene bilayer flake in a model nanocomposite. (a) Overall band shift for the bilayer, (b) Details of the band for the bilayer, (c) Shift with strain of the bands fitted to a single peak, (d) The variation with strain of the FWHM of the bands fitted to a single peak.

S1.3 Band shift in the central region of a trilayer flake

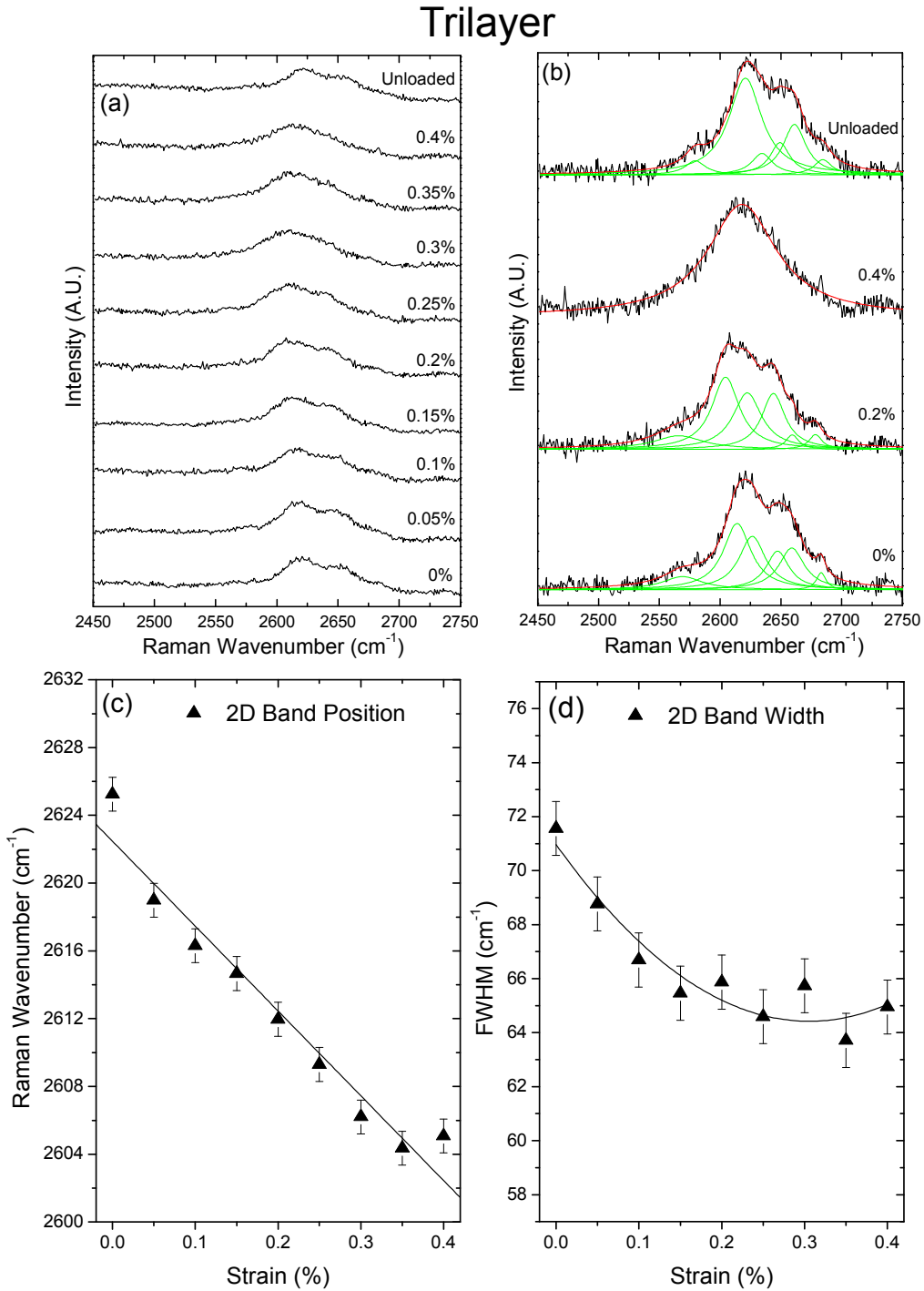


Figure S3. Shift of the 2D Raman band with strain for a graphene trilayer flake in a model nanocomposite. (a) Overall band shift for the trilayer, (b) Details of the band for the trilayer, (c) Shift with strain of the bands fitted to a single peak, (d) The variation with strain of the FWHM of the bands fitted to a single peak.

S1.4 Band shift in the central region of a few-layer flake

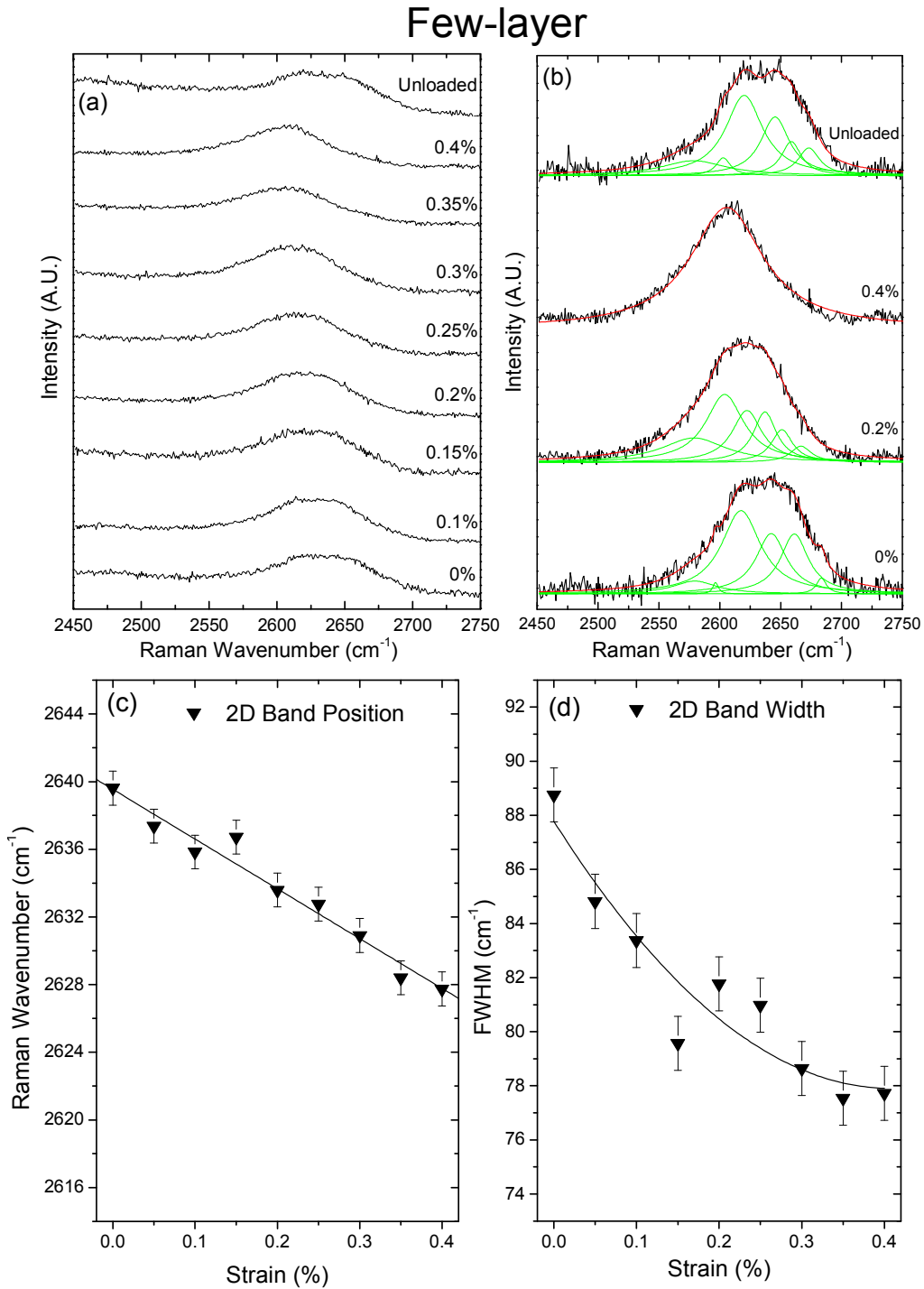


Figure S4. Shift of the 2D Raman band with strain for a few-layer graphene flake in a model nanocomposite. (a) Overall band shift for the flake, (b) Details of the band for the flake, (c) Shift with strain of the bands fitted to a single peak, (d) The variation with strain of the FWHM of the bands fitted to a single peak.

S1.5 Mapping across a trilayer flake

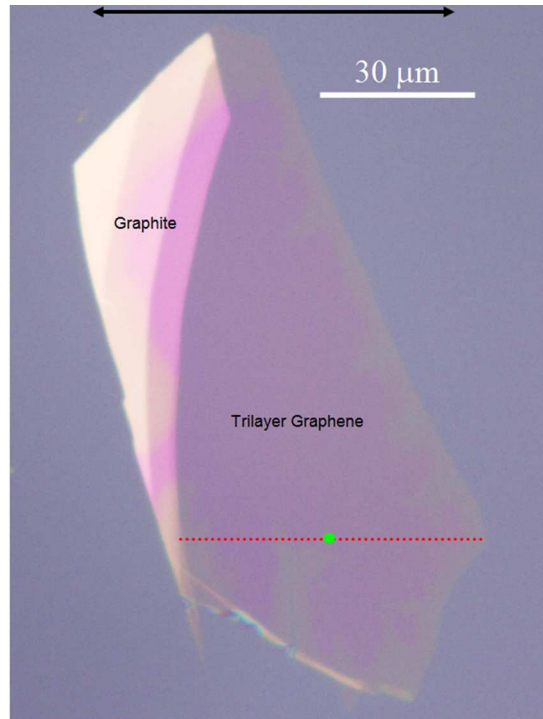


Figure S5. Optical micrograph of a flake in a model composite containing a large graphene trilayer region. The green spot shows the area used for the overall Raman band shift measurements and red dotted line is the region mapped at the different strain levels. The strain was in the horizontal direction as shown by the black arrow.

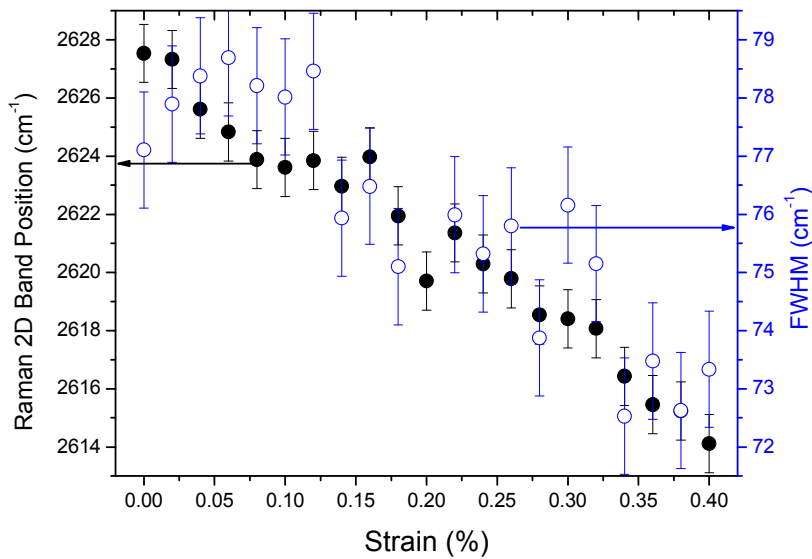


Figure S6. Variation of position and FWHM of the 2D band for the middle of the flake (green spot) shown in Figure S5. The shift of the 2D band to lower wavenumber accompanied by band narrowing can be clearly seen.

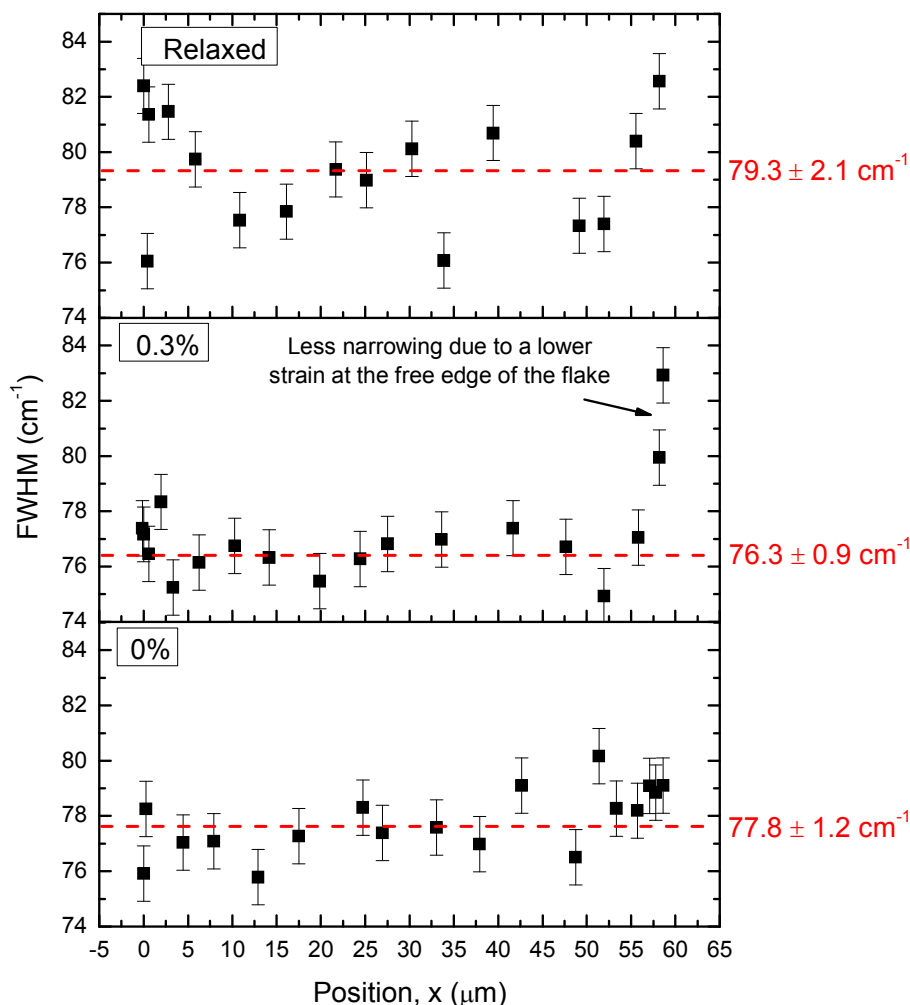


Figure S7. Variation of the FWHM of the 2D band along the red dotted line in the trilayer region of the flake shown in Figure S5 at different levels of applied strain, 0%, 0.3% and relaxed.

Figure S7 shows the variation of FWHM along the trilayer flake at different levels of applied strain. In the undeformed state (0%) the average FWHM across the flake is 77.8 cm^{-1} with a standard deviation of 1.2 cm^{-1} . At 0.3% strain the FWHM narrows to $76.3 \pm 0.9 \text{ cm}^{-1}$ over the central region of the flake. The values of FWHM are higher at the ends of the flake as a result of the lower strain at the free edges, as has been found before¹. When the strain on the flake is relaxed after being loaded up to 0.4% strain (Figure S6) the average FWHM increases to $79.3 \pm 2.1 \text{ cm}^{-1}$. The larger standard deviation in the relaxed state could be due to local fluctuations in strain due to the presence of defects in the flake that have not disappeared completely upon unloading.

S2. Loss of Bernal Stacking

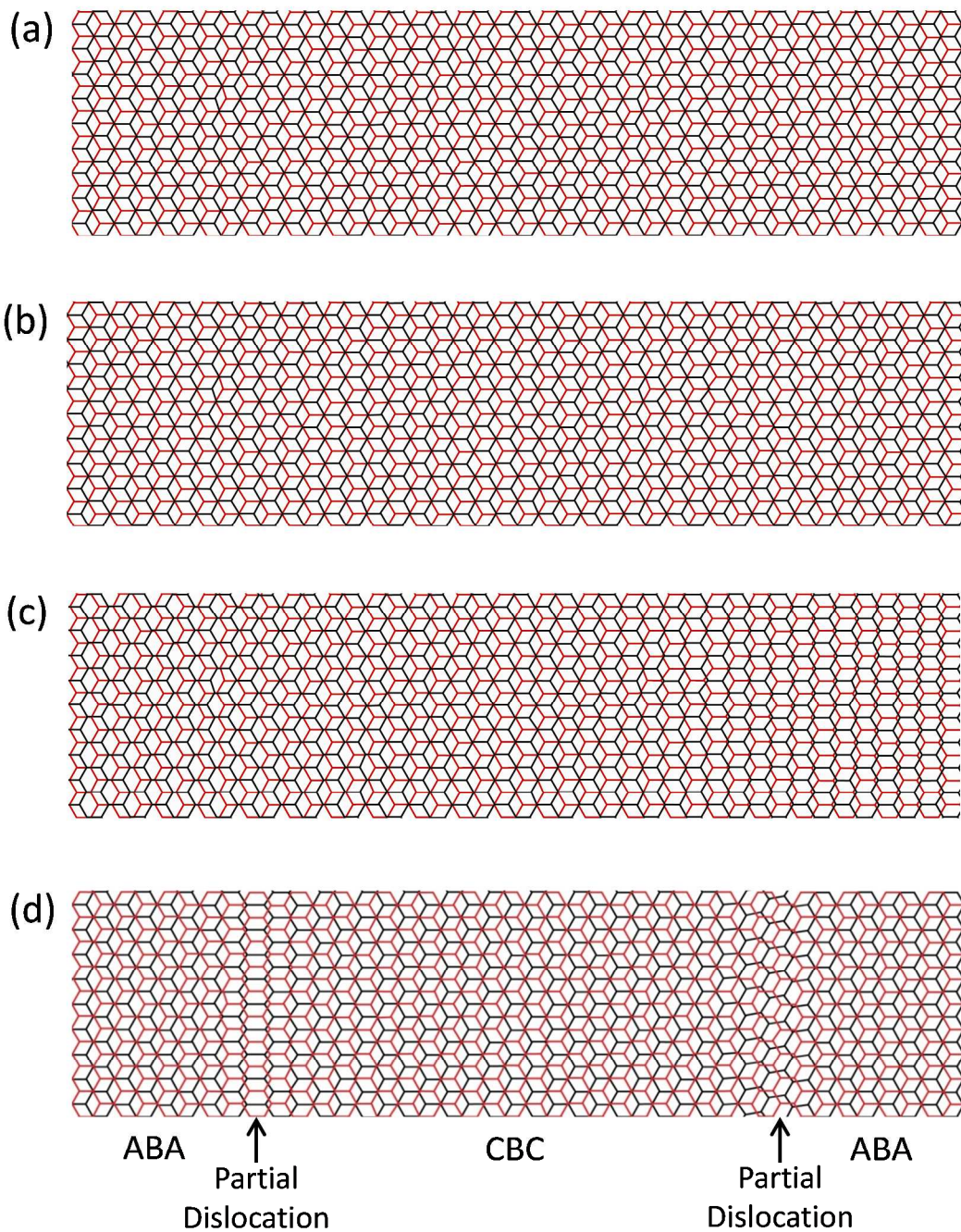


Figure S5. Bernal stacked trilayer graphene lattice structure. (a) Undeformed material. (b) Deformed structure showing affine deformation in all layers at 1% strain (b) (c) Deformed structure with the middle B layer relaxed to 0% strain showing a stacking fault. (d) Deformed structure showing an undeformed B layer and the formation of two partial dislocations and a stacking fault in the outer layers (the top and bottom A layers are shown with the same deformation for clarity). The left-hand side dislocation has edge character and the right-hand side one is mixed edge and screw. (The A layers are colored black and the B layer is colored red).

S3. Energetics of the Loss of Bernal Stacking

S3.1 Loss of Bernal Stacking for Few-layer Graphene

For N layers of graphene under deformation, the elastic stored energy U_s of the middle layers is given by

$$U_s = (N - 2) \frac{1}{2} E_g e_g^2 V \quad (\text{S1})$$

where E_g is the Young's modulus of the graphene (~ 1 TPa), e_g is the elastic strain in the graphene and V is the volume of a single graphene layer.

The volume of the graphene layer is given by

$$V = l_0 w_0 d \quad (\text{S2})$$

where l_0 , w_0 and d are the length, width and thickness of the graphene layer ($d = 0.34$ nm).

Upon the loss of Bernal stacking, the increase in van der Waals energy U_{SF} by forming N non-AB Bernal-stacked layers is

$$U_{\text{SF}} = (N - 1) \Delta u (l_0 w_0 / A) \quad (\text{S3})$$

where Δu is the stacking fault energy per atom of the non-Bernal stacked graphene, $A = \frac{3}{4} \sqrt{3} a^2$ is the area per atom in the graphene lattice and $a (= 0.142$ nm) is the C-C bond length.

When the stored elastic energy U_s exceeds the stacking fault energy U_{SF} , the loss of Bernal stacking will become energetically favorable. Thus the critical situation is when $U_s = U_{\text{SF}}$ which leads to

$$\Delta u = \frac{3}{8} \frac{(N - 2)}{(N - 1)} E_g e_g^2 d \sqrt{3} a^2 \quad (\text{S4})$$

As discussed in the text, the loss of Bernal stacking normally occurs at around 0.4% strain. In the simplest case of trilayer graphene ($N = 3$) it is possible use this equation to estimate the stacking fault energy of graphene as

$$\Delta u = 0.22 \text{ meV/atom} \quad (\text{S5})$$

This value is in agreement with that obtained by Shibuta and Elliott⁴ who showed that for the interaction between two graphene sheets with a turbostratic orientational relationship, the loss of AB stacking through either rotation or displacement of the two sheets relative to each other, the energy gap between AB and AA stacking is the order of 0.36 meV/atom.

S3.2 Dislocation Energetics

There is accumulated evidence from studies upon graphite^{5,6} that such deformation will lead to arrays of basal plane stacking faults and partial dislocations.

The Burgers vector of the partial dislocation is

$$\mathbf{b} = x\mathbf{c} \quad (\text{S6})$$

where \mathbf{c} is the Burgers vector of the complete dislocation and x is the fraction of \mathbf{c} . Along the armchair direction of graphene $|\mathbf{c}| = 3a$, where $a = 0.142$ nm is the bond length.

In the vicinity of a dislocation, the loss of perfect AB stacking leads to an increase of the van der Waals energy by $2\Delta uwl/A$ where Δu is the stacking fault energy difference per atom, and w and l are the width and length of the partial dislocation and A is the area per atom in the graphene lattice.

The elastic energy due to the deformation around a partial dislocation can be written approximately as

$$\frac{1}{2} E_g (b/w)^2 lwd$$

Hence the total energy for the loss of Bernal stacking is

$$U_T = 2\Delta uwl/A + \frac{1}{2} E_g (b/w)^2 lwd \quad (\text{S7})$$

This energy is minimised in terms of the dislocation width when

$$\frac{dU_T}{dw} = 2\Delta uwl/A + \frac{1}{2} E_g (b/w)^2 lwd = 0 \quad (\text{S8})$$

which leads to the optimum width of the partial dislocation as

$$w = b\sqrt{E_g ad / 4\Delta u} \approx 250b \approx 40 \text{ nm} \quad (\text{S9})$$

For an elongation of 0.4%, the distance between to neighbouring partial dislocations is given by $(0.142/0.004)$ nm ~ 35 nm. This means that the separation of the partial dislocations will be of the order of their width and that regular stacking will be effectively lost in the whole area.

References

1. Gong, L.; Kinloch, I. A.; Young, R. J.; Riaz, I.; Jalil, R.; Novoselov, K. S. Interfacial Stress Transfer in a Graphene Monolayer Nanocomposite. *Adv. Mater.*, **2010**, *22*, 2694-2697.
2. Young, R. J.; Gong, L.; Kinloch, I. A.; Riaz, I.; Jalil R.; Novoselov, K. S., Strain Mapping in a Graphene Monolayer Nanocomposite, *ACS Nano*, **2011**, *5*, 3079-3084.
3. Gong, L.; Young, R. J.; Kinloch, I. A.; Riaz, I.; Jalil R.; Novoselov, K. S., Optimizing the Reinforcement of Polymer-Based Nanocomposites by Graphene, *ACS Nano*, **2012**, *6*, 2086-2095.
4. Shibuta, Y.; Elliott, J. A. Interaction Between Two Graphene Sheets with a Turbostratic Orientational Relationship, *Chem. Phys. Lett.*, **2011**, *512*, 146-150.
5. Amelinckx, S.; Delavignette, P. Electron Optical Study of Basal Dislocations in Graphite, *J. Appl. Phys.*, **1960**, *31*, 2126-2135.
6. Baker, C.; Kelly, A. The Effect of Neutron Irradiation on the Elastic Moduli of Graphite Single Crystals, *Phil Mag.*, **1964**, *9*, 927-951.